Synthesis, Self-assembly Behaviours and Multivalent Glycosidase Inhibition Effect of Deoxynojirimycin Modified Perylene Bisimide Derivative

Juan-Juan Li, [a] Ke-Rang Wang,* [a] Ren-Feng Li, [b] Jian-Xing Yang, [a] Min Li, [a] Hong-Xin Zhang,[c] Zhi-Ran Cao, [b] and Xiao-Liu Li*[a]

[a] Key Laboratory of Medicinal Chemistry and Molecular Diagnosis (Ministry of Education), Key laboratory of Chemical Biology of Hebei Province, College of Chemistry and Environmental Science, Hebei University, 071002, Baoding, P. R. China

[b] Department of Immunology, School of Basic Medical Science, Hebei University, 071002, Baoding, P. R. China.

[c] Medical comprehensive experimental center of Hebei University, Baoding, 071000, China.

E-mail: kerangwang@hbu.edu.cn; lixl@hbu.edu.cn.

S1. Experimental section

Determination of the standard curve of p-nitrophenol (PNP) in the citric acid-phosphate buffer (pH 5.5, 0.1 mmol), in the citric acid-phosphate buffer (pH 6.8, 0.1 mmol), and in the citric acid-phosphate buffer (pH 7.3, 0.1 mmol).

p-Nitrophenol (PNP) (13.9 mg, 0.1 mmol) was dissolved in 5 mL of the citric acid-phosphate buffer (pH 5.5, 0.1 mmol) or the PBS buffer (pH 6.8, 0.1 mmol), or the PBS buffer (pH 7.3, 0.1 mmol), the final concentration was 20 mmol/L, and then which was diluted to the final concentrations of 0.5, 1.0, 2.0, 4.0, 8.0, 16.0, 32.0, 64.0, 128.0 and 256.0 μmol/L by the buffer solution, respectively. 100 μL of the above standard solutions (0.5, 1.0, 2.0, 4.0, 8.0, 16.0, 32.0, 64.0, 128.0 and 256.0 μmol/L) was plated in 96-well microassay culture plates, and then 100 μL of Na_2CO_3 solution was added, the plates were mixed for 3 min. The optical density of each well was then measured on a microplate spectrophotometer at a wavelength of 405 nm. The reaction dynamics of the standard curve of p-nitrophenol (PNP) or o-Nitrophenol (ONP) were fitted by line formula (y = Ax + B), the slopes (K_{slope}) were obtained.

Glycosidase Inhibitory Activities of PBI-DNJ

Inhibition assay was determined by spectrophotometrically measuring the residual hydrolytic activities of the different glycosidases against the respective p-nitro-phenyl-α-glycopyranoside, or β-D-glycopyranoside, or o-nitro-phenyl-α- glycopyranoside, in the presence of the assemblies of **PBI-DNJ** or the control drug. The glycosidase inhibitory activities of **PBI-DNJ** were performed in 96-well microassay culture plates with blank group, control group, experimental blank group and experimental group, 3 parallel experiments for per group.

Firstly, 20 μL of the citric acid-phosphate buffer (pH 5.5, 0.1 mmol) was added to the 96-well plates, then 10 μL of α-mannosidase (0.2U/mL) was added to per well. After that, various concentrations of **PBI-DNJ** (20 μL of 5, 10, 20, 40, 80 and 160 μmol/L) were added the 96-well plates for the final concentrations of 0, 0.5, 1.0, 2.0, 4.0, 8.0 and 16.0 μmol/L. The mixture was well mixed for 3 min, and incubated at 37 °C in a 5% CO_2 incubator for 10 min. Then, reaction substrates of 4-nitrophenyl α-D-mannopyranoside (50 μL of 0.5, 1.0, 2.0, 4.0, 8.0 and 16.0 mmol/L) were added, mixed for 3 min, and incubated at 37 °C in a 5% CO_2 incubator for 20 min. At last, 100 μL of Na_2CO_3 (1 mol/L) was added, mixed for 3 min. The absorbance of the reaction mixture was determined at 405 nm with a microplate spectrophotometer.

According to the standard curves of p-nitrophenol (PNP) in the citric acid-phosphate buffer (pH 5.5, 0.1 mmol), the inhibition concentration of PNP was obtained by coupling of the K_{slope} with the changes of the absorption intensity for the experimental blank group and experimental group, then the reaction speed of PNP with α-mannosidase was obtained by against the reaction time. The reaction speed (V) was obtained by the concentration of PNP against the reaction time (20 min). Then plot of 1/V against 1/S, the slopes of various concentrations of **PBI-DNJ** were obtained. The V was the reaction speed of PNP with α-mannosidase in presence of various concentrations of **PBI-DNJ**. The S was the concentrations of PNP added in the 96-well plates. After that, the K_i value of **PBI-DNJ** with α-mannosidase was obtained by plot of the concentrations of **PBI-DNJ** against the slopes obtained by the above results by the Lineweaver-Burk method. The K_i values and enzyme inhibition mode were obtained

from the slope of Linewaver-Burk plots and double reciprocal analysis using Origin 8.0.

The K_i values of **PBI-DNJ** against the other glycosidases were obtained by the similar method. 20 μL of the citric acid-phosphate buffer (pH 5.5, 0.1 mmol) was added to the 96-well plates, then 10 μL of α-galactosidase (0.2U/mL), or α-glucosidase (50 U/mL), was added to per well. After that, various concentrations of **PBI-DNJ** (20 μL of 100, 200, 400, 600 and 800 μmol/L for α-galactosidase activity; or 20 μL of 10, 20, 40 and 80 μmol/L for α-glucosidase activity) were added to the 96-well plates for the final concentrations of α-galactosidase activity (0, 10, 20, 40, 60 and 80 μmol/L) and α-glucosidase activity (0, 1, 2, 4 and 8 μmol/L). The mixture was well mixed for 3 min, and incubated at 37 °C in a 5% CO_2 incubator for 10 min. Then, 50 μL of the reaction substrates (0.5, 1.0, 2.0, 4.0, 8.0 and 16.0 mmol/L) for 4-nitrophenyl α-D-galactopyranoside, or 4-nitrophenyl α-D-glucopyranoside were added, mixed for 3 min, and incubated at 37 °C in a 5% CO_2 incubator for 20 min. At last, 100 μL of Na_2CO_3 (1 mol/L) was added, mixed for 3 min. The absorbance of the reaction mixture was determined at 405 nm with a microplate spectrophotometer.

TEM Measurements.

The solution of **PBI-DNJ** under different pH values in TEM experiment was corrected by HCl (2 mol·L^{-1}) or NaOH (1 mol·L^{-1}). **PBI-DNJ** was dissolved in water at the pH value of 6.69 under the concentration of 1×10^{-4} M. 0.27 mL of HCl (2 mol·L^{-1}) solution was dropped to the **PBI-DNJ** solution, the final pH value was 3.01. On the other hand, 30 μL of NaOH (1 mol·L^{-1}) solution was dropped to the **PBI-DNJ** solution, the final pH value was 6.99. The pH value of the solution was determined by a pH meter. A 1.0×10^{-4} M of **PBI-DNJ** solution under the pH values of 3.0 and 7.0 was dropped onto a copper grid. The grid was then air-dried for 2 days. The samples were examined by a high-resolution TEM (Tecnai G^2 F20 (FEI)) operating at an accelerating voltage of 200 keV.

Cell Viability Assay.

Compound **PBI-DNJ** was dissolved in PBS buffer and diluted to the required concentration with culture medium. The cytotoxicity was studied by a MTT assay.

Briefly, cells were plated in 96-well microassay culture plates (7.0×10^3 cells per well) and grown overnight at 37 °C in a 5% CO_2 incubator. Compound **PBI-DNJ** was then added to the wells to achieve final concentrations ranging from 10^{-7} to 10^{-4} M. Wells containing culture medium without cells were used as control blanks; wells containing culture medium was used as positive control. The plates were incubated at 37 °C in a 5% CO_2 incubator for 48 h. Upon completion of the incubation, stock MTT dye solution (20 μL, 5 mg/μL) was added to each well. After 4 h incubation, Dimethyl Sulfoxide (DMSO, 150 μL) was added to solubilize the MTT formazan. The optical density of each well was then measured on a microplate spectrophotometer at a wavelength of 490 nm.

General Procedures for Glycosidase Inhibition Assay.

Inhibition assay was determined by spectrophotometrically measuring the residual hydrolytic activities of the different glycosidases against the respective p-nitro-phenyl-α- or β-D-glycopyranoside, in the presence of the assemblies of **PBI-DNJ** or the control drug. The reactions were initiated upon addition of glycosidase enzymes to the solutions of the substrates in the absence or presence of various concentrations of glycosidase inhibitors. After the mixture was incubated for 10~30 min at 37 ºC, the reaction was quenched by addition of 1 M Na_2CO_3. The absorbance of the reaction mixture was determined at 405 nm with a microplate spectrophotometer. The K_i values and enzyme inhibition mode were obtained from the slope of Linewaver-Burk plots and double reciprocal analysis using Origin 8.0.

S2. Additional Figures and Table

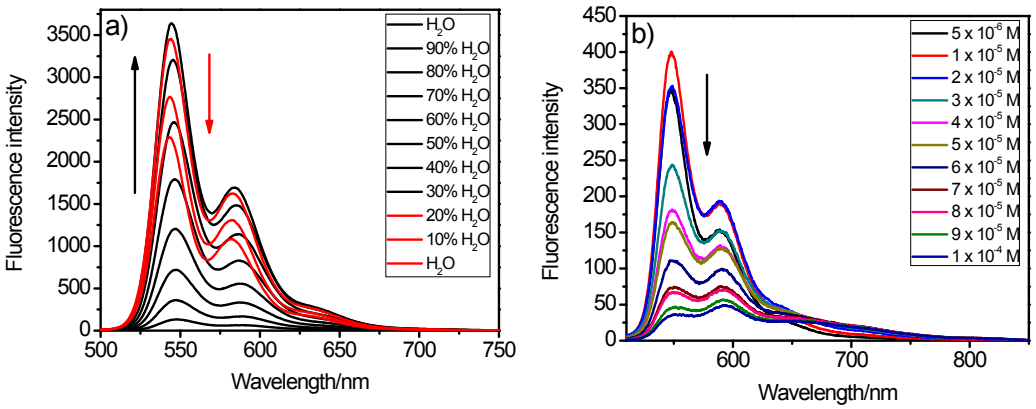

Fig. S1 Solvent-dependent (DMSO-H_2O, 1 × 10^{-5} M, λ_{ex} = 490 nm, a) and concentration-dependent (λ_{ex} = 500 nm, b) fluorescence spectra of **PBI-DNJ** in water.

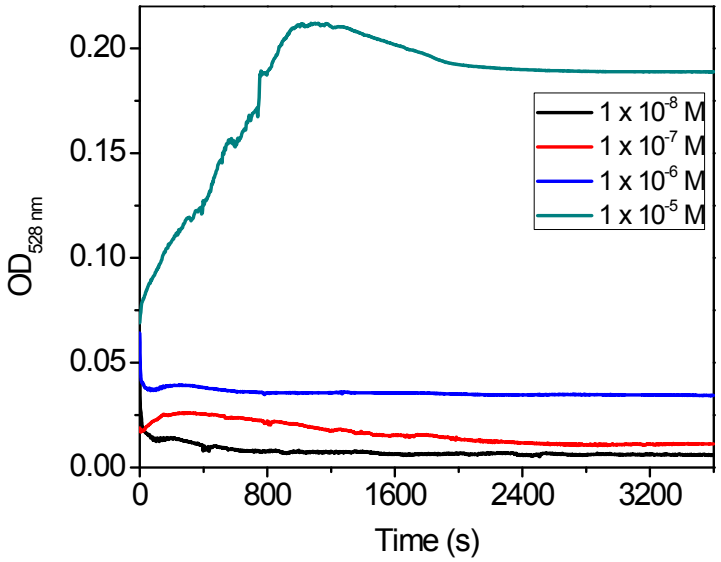

Fig. S2 Self-assembled dynamic plots of **PBI-DNJ** in water at the concentrations of 1 × 10^{-8} M, 1 × 10^{-7} M, 1 × 10^{-6} M and 1 × 10^{-5} M.

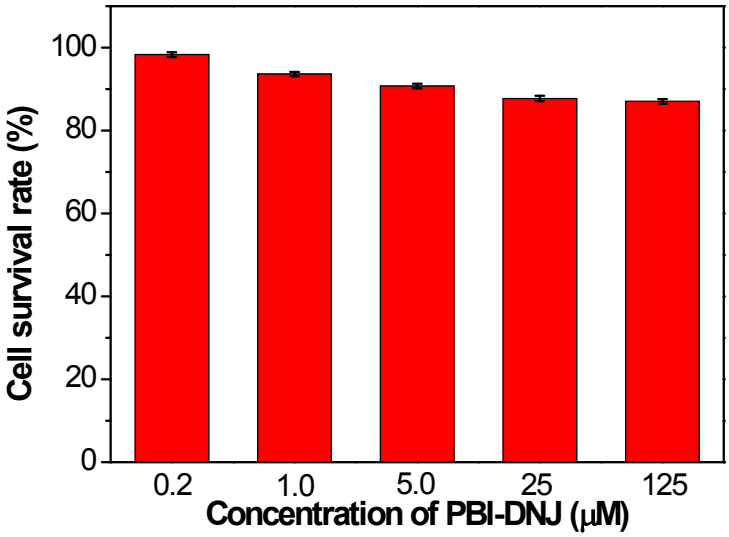

Fig. S3 Cell survival rate of **PBI-DNJ** against HKC 60 cells at different concentrations.

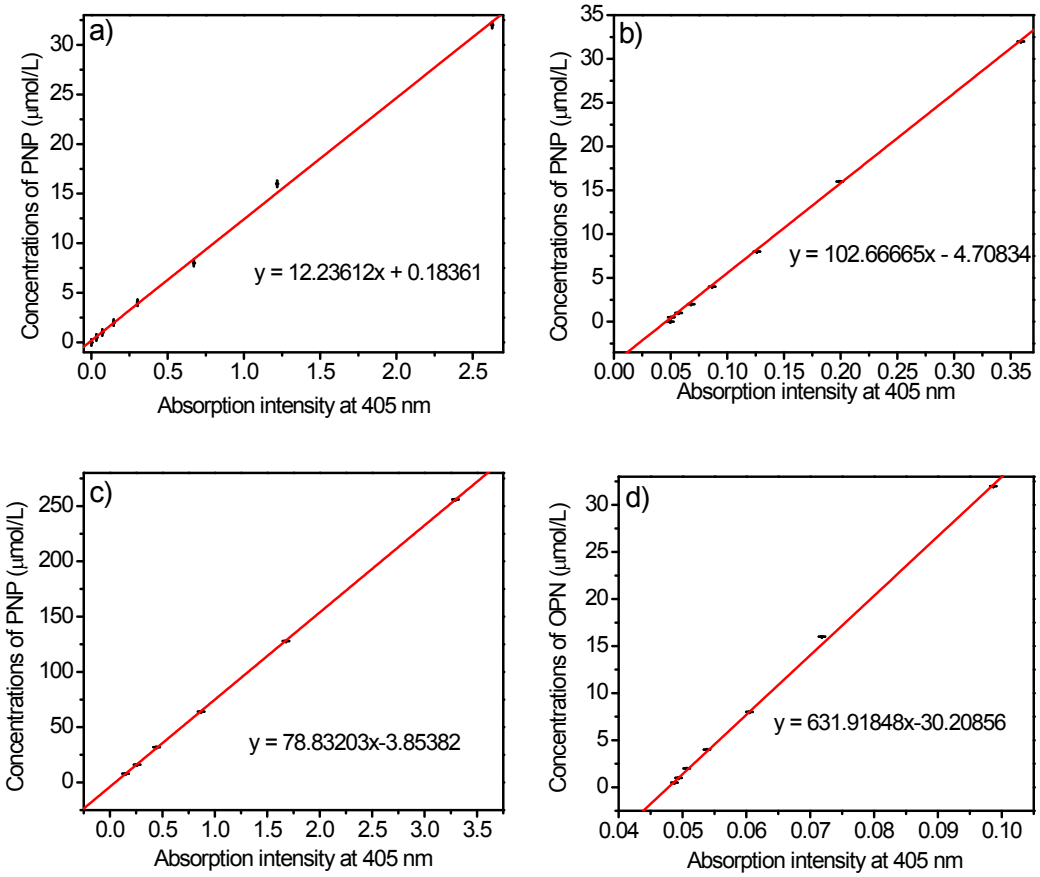

Fig. S4 The standard curves of p-nitrophenol (PNP) in the citric acid-phosphate buffer (pH 5.5, 0.1 mmol) (a), in the PBS buffer (pH 6.8, 0.1 mmol) (b) and in the PBS buffer (pH 7.3, 0.1 mmol) (c), and (d) the standard curve of o-nitrophenol (ONP) in the PBS buffer (pH 7.3, 0.1 mmol).

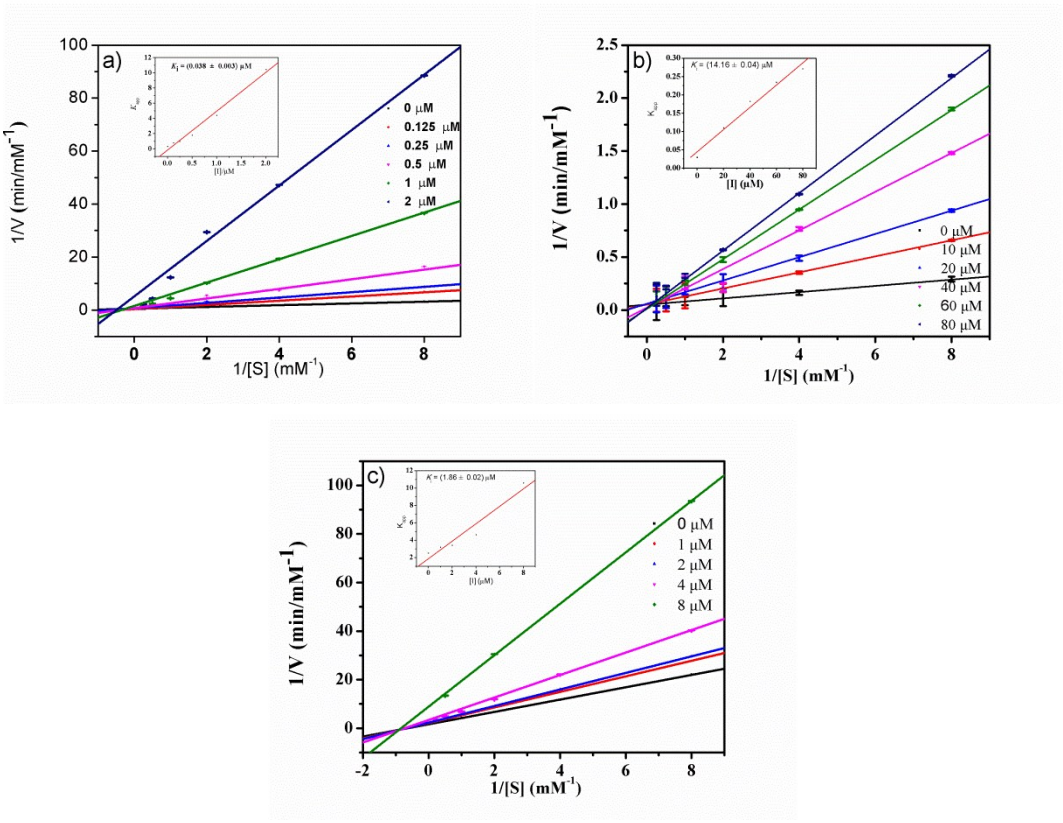

Fig. S5 Lineweaver-Burk plot for K_i determination of **PBI-DNJ** against *α*-mannosidase (*Jack bean*, a), *α*-galactosidase (*green coffee beans*, b) and *α*-glucosidase (*aspergillus niger*, c).

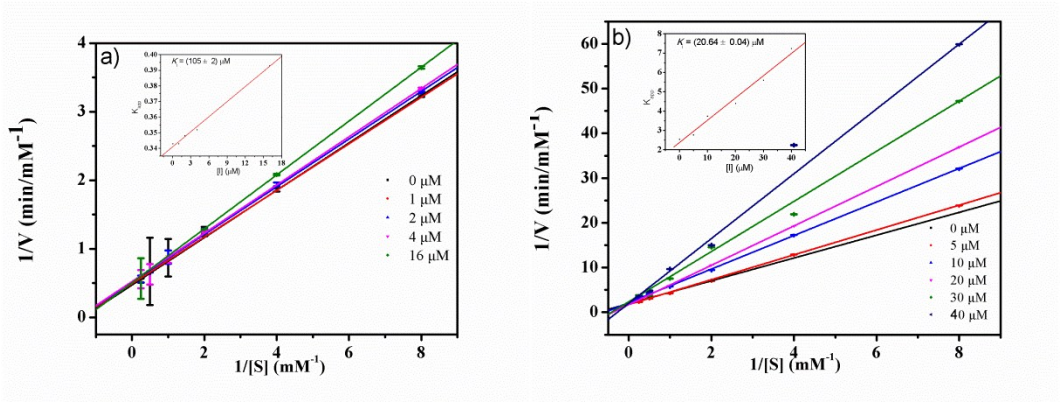

Fig. S6 Lineweaver-Burk plot for K_i determination of miglitol against *α*-mannosidase (*Jack bean*, a) and *α*-glucosidase (*aspergillus niger*, b).

Table S1. Glycosidase inhibitory activities (K_i, μM) of **PBI-DNJ** and the other multivalent glycosidase inhibitors reported in references against *α*-mannosidase (*jack bean*).

Glycosidase	K_i (μM)	valency	RIP[a]	RIP/n[b]

Monomer DNJ		1	1	1
PBI-DNJ/Monomer DNJ	0.038/400[1]	6	10526	1754
PBI-DNJ/Monomer DNJ	0.038/270[2]	6	7105	1184
Porphyrin-DNJ[1]/Monomer DNJ	0.5/400	4	800	200
Fullerene-12DNJ[3]/Monomer DNJ	0.15/322	12	2147	179
ICDCs[4]/Monomer DNJ	0.022/322	14	8546	610
Fullerene-120DNJ[5]/Monomer DNJ	0.0018/204	120	113333	944
Fullerene-108DNJ[5]/Monomer DNJ	0.0072/204	108	28333	262
Cyclopeptoid-36DNJ[6]/Monomer DNJ	0.0011/188	36	170909	4747
Cyclopeptoid-48DNJ[6]/Monomer DNJ	0.0011/188	36	170909	3560
Copolymer-DNJ[7]**/Monomer DNJ**	0.15/516	25	3440	206

[a] Relative inhibition potency over Monomer DNJ.

[b] Relative inhibition potency over Monomer DNJ/per DNJ unit.

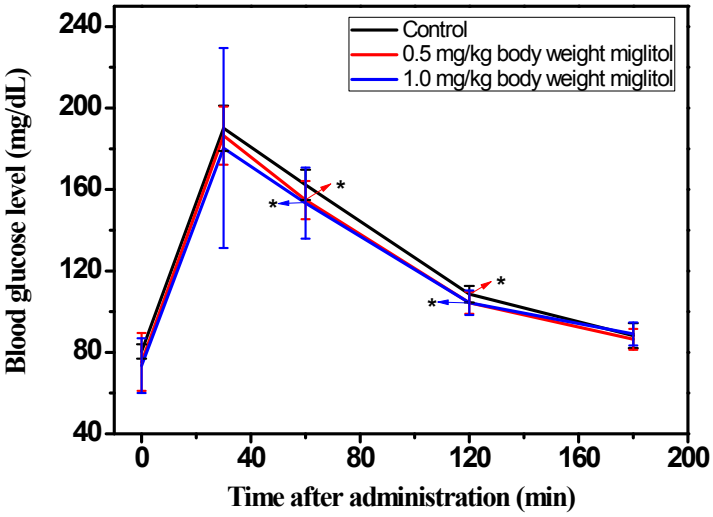

Fig. S7 The hypoglycaemic effects of miglitol on blood glucose level in mice, maltose (2 g·kg^{-1} of body weight) was orally administered to mice along with miglitol (0.5 and 1.0 mg·kg^{-1} of body weight). Each value represents the mean ± SEM (n = 5), $*p < 0.05$ vs. the control results.

Table S2. The body weight before and after oral sugar tolerance test in mice for 7 days.

	NO.	Control (Maltose)	0.5 mg·kg^{-1} (**PBI-DNJ**)	1.0 mg·kg^{-1} (**PBI-DNJ**)
Before of oral sugar tolerance test	1	17 g	17 g	17 g
	2	17 g	17 g	17 g
	3	17 g	17 g	17 g
	4	18 g	17 g	18 g
	5	18 g	17 g	18 g
After of oral sugar tolerance test for 7 days	1	19 g	19 g	19 g
	2	22 g	21 g	28 g
	3	18 g	18 g	22 g
	4	18 g	18 g	18 g
	5	19 g	19 g	19 g

S3. Additional Figures of the NMR and HRMS

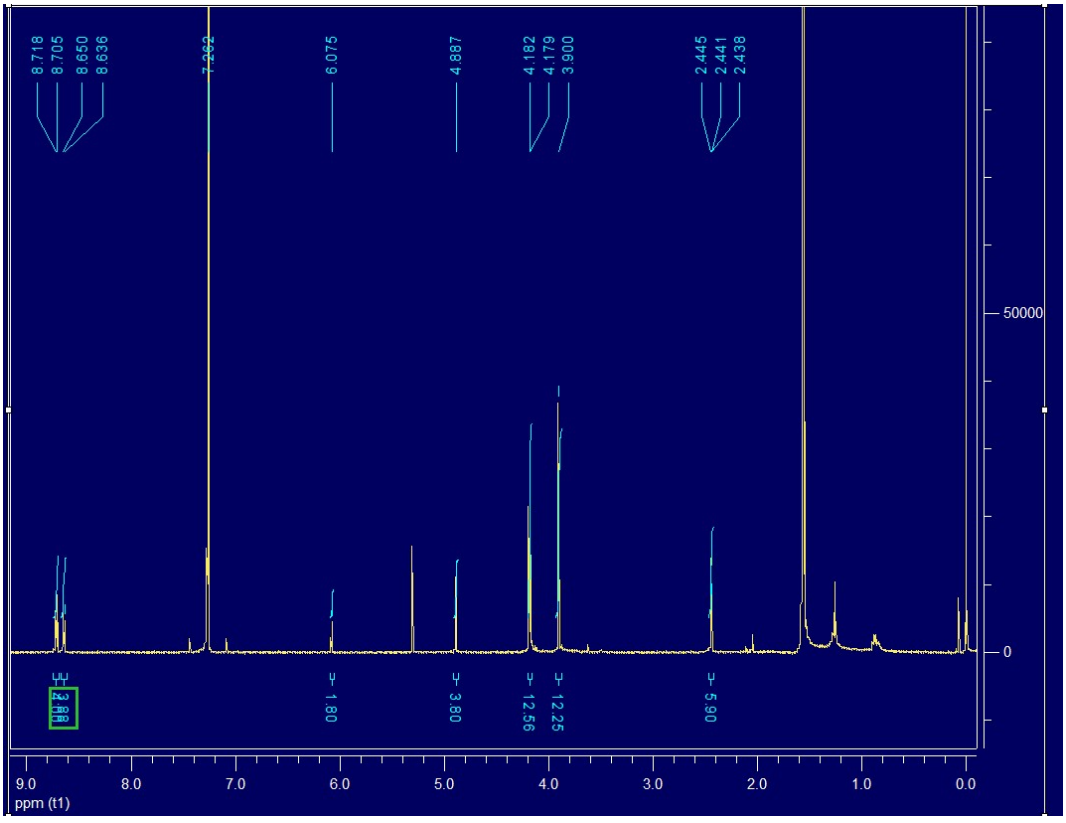

Fig. S8 ^{1}H NMR of compound **3** ($CDCl_3$, 600 MHz).

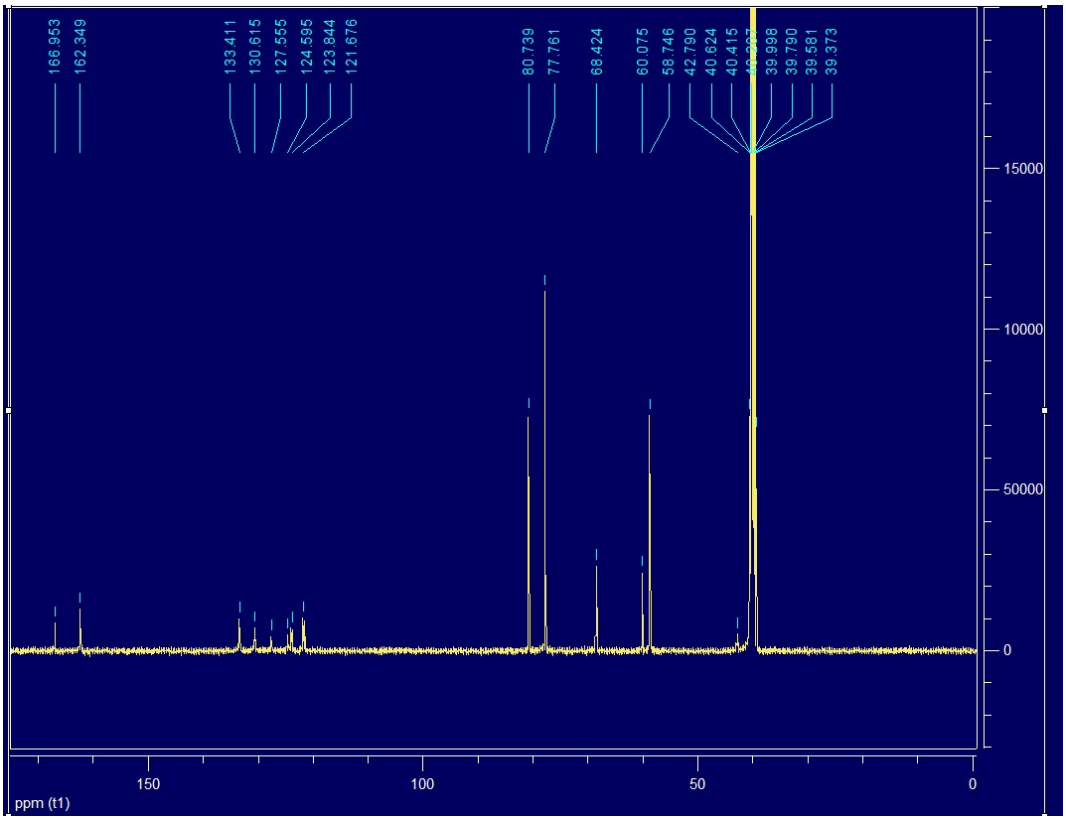

Fig. S9 ^{13}C NMR of compound **3** ($CDCl_3$, 100 MHz).

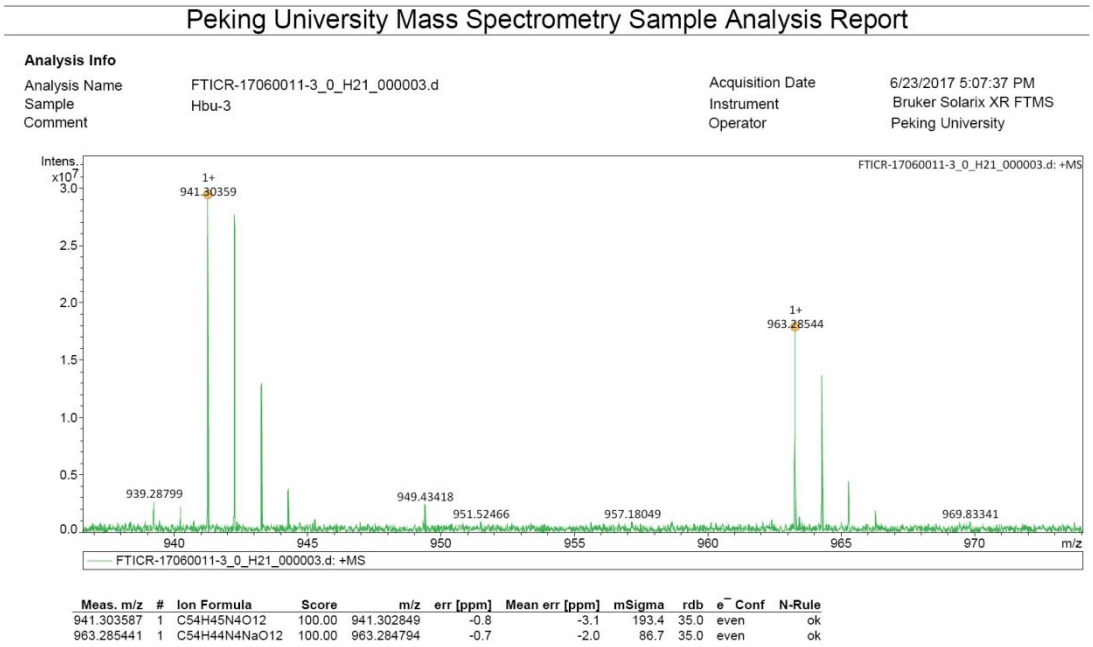

Meas. m/z	#	Ion Formula	Score	m/z	err [ppm]	Mean err [ppm]	mSigma	rdb	e¯ Conf	N-Rule
941.303587	1	C54H45N4O12	100.00	941.302849	-0.8	-3.1	193.4	35.0	even	ok
963.285441	1	C54H44N4NaO12	100.00	963.284794	-0.7	-2.0	86.7	35.0	even	ok

Fig. S10 HRMS of compound **3**.

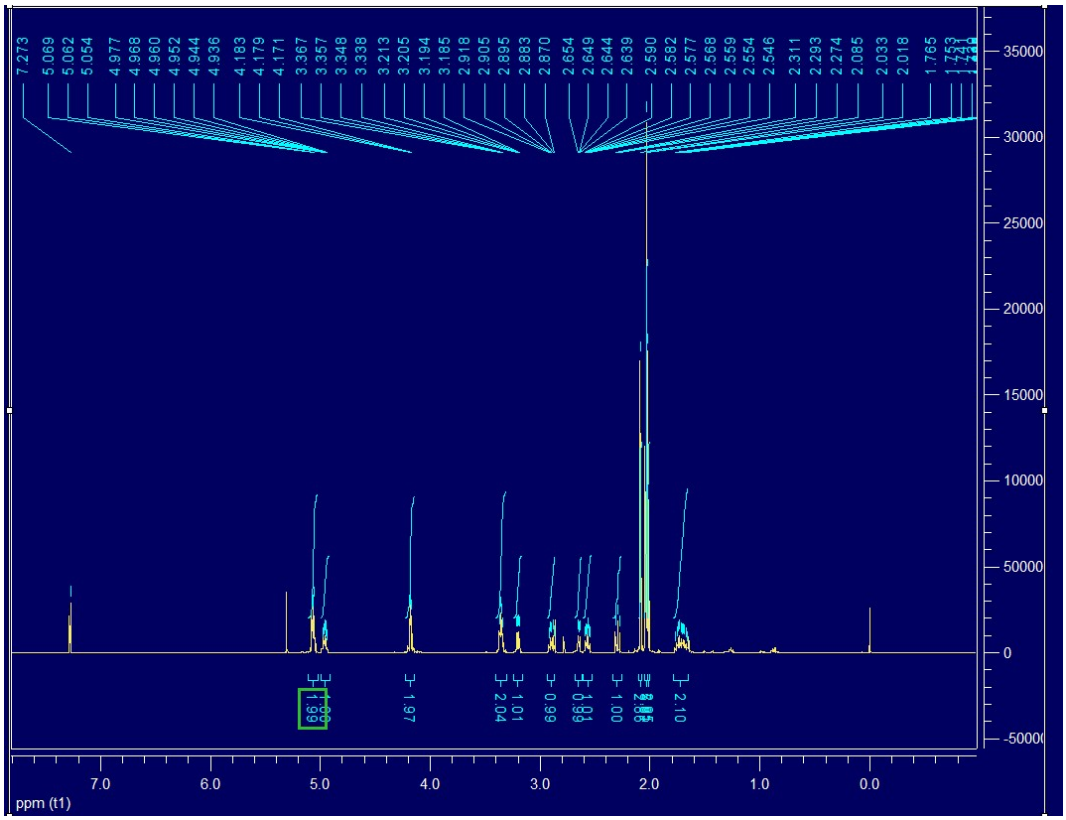

Fig. S11 ^{1}H NMR of compound **4** ($CDCl_3$, 600 MHz).

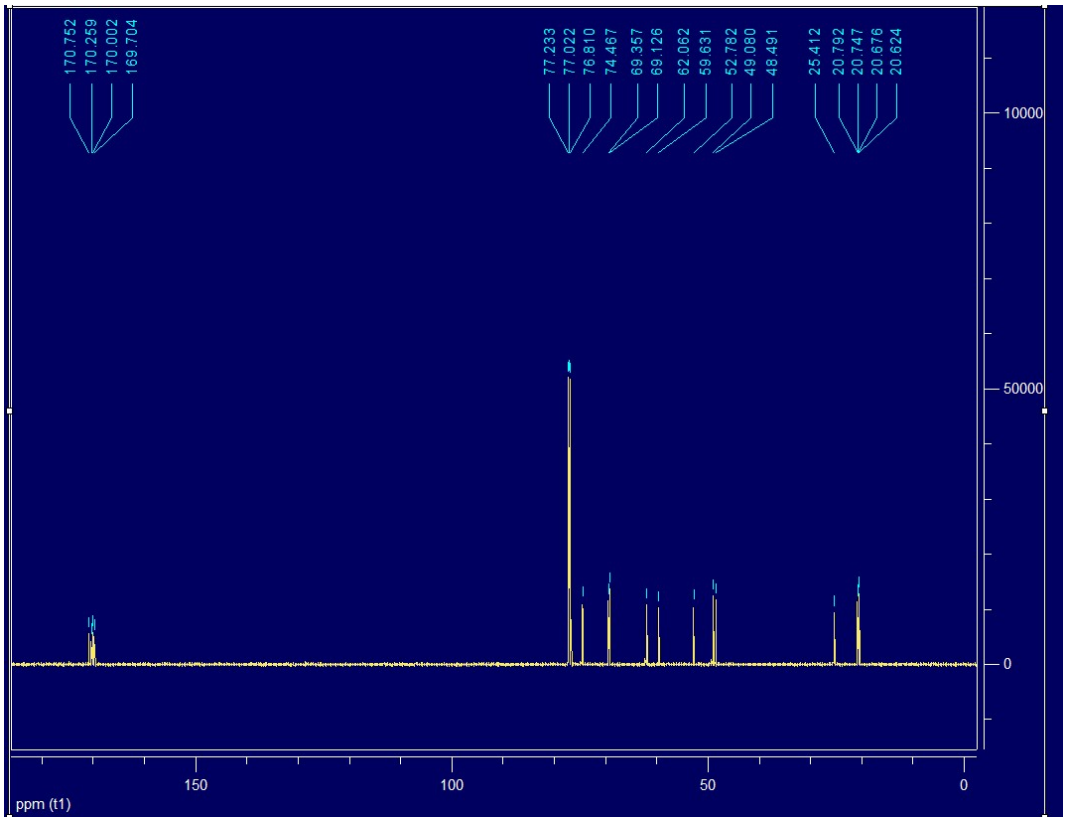

Fig. S12 ^{13}C NMR of compound **4** ($CDCl_3$, 150 MHz).

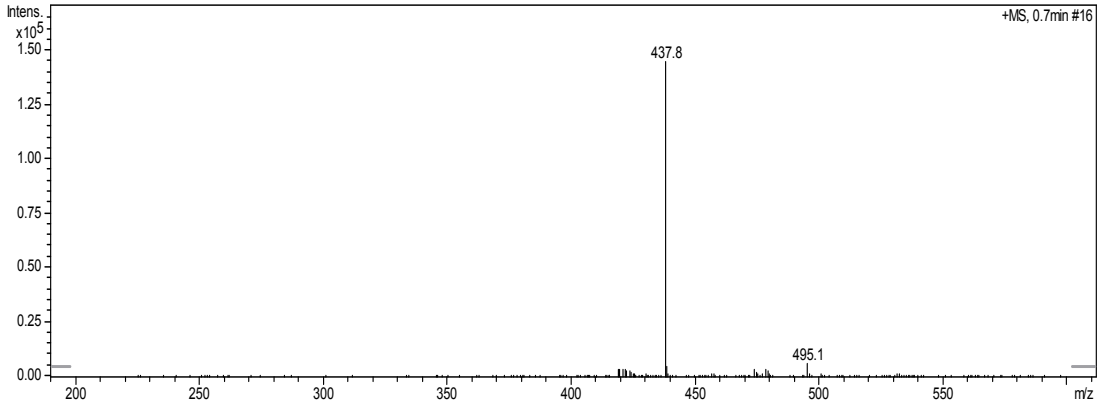

Fig. S13 MS (ESI) of compound **4**.

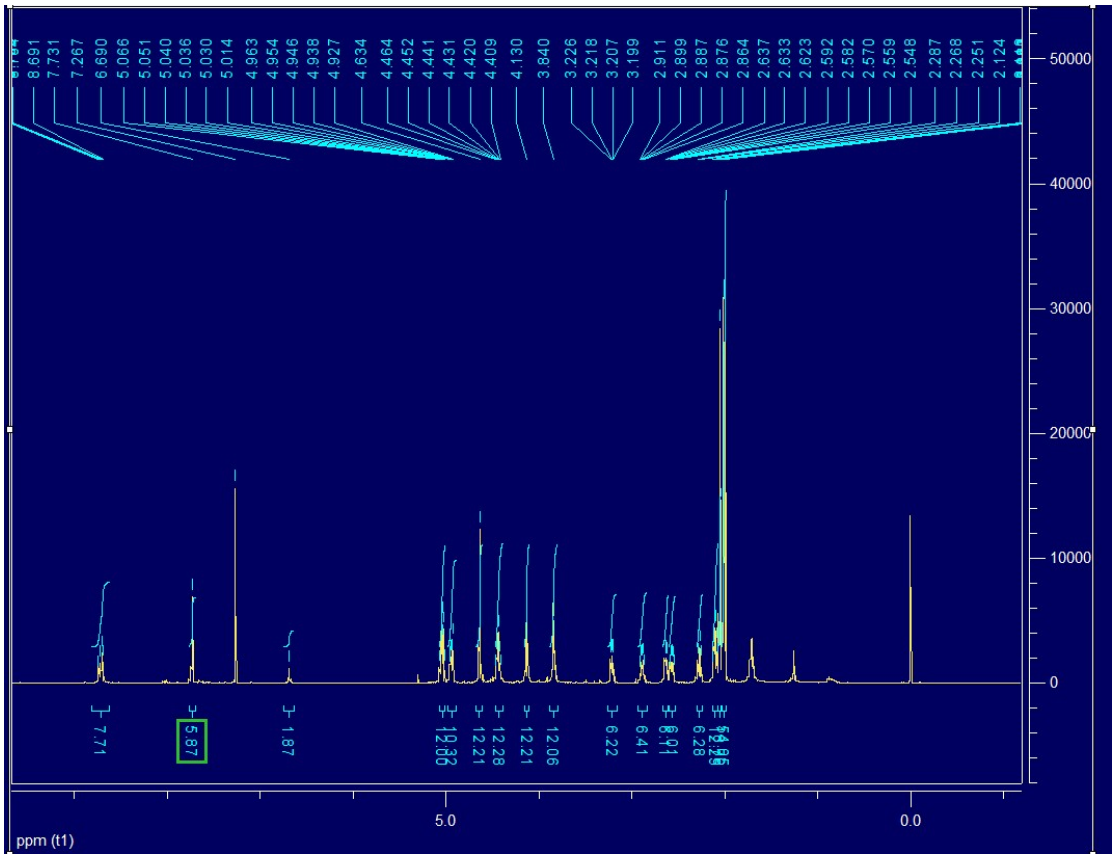

Fig. S14 ^{1}H NMR of compound **PBI-AcDNJ** ($CDCl_3$, 600 MHz).

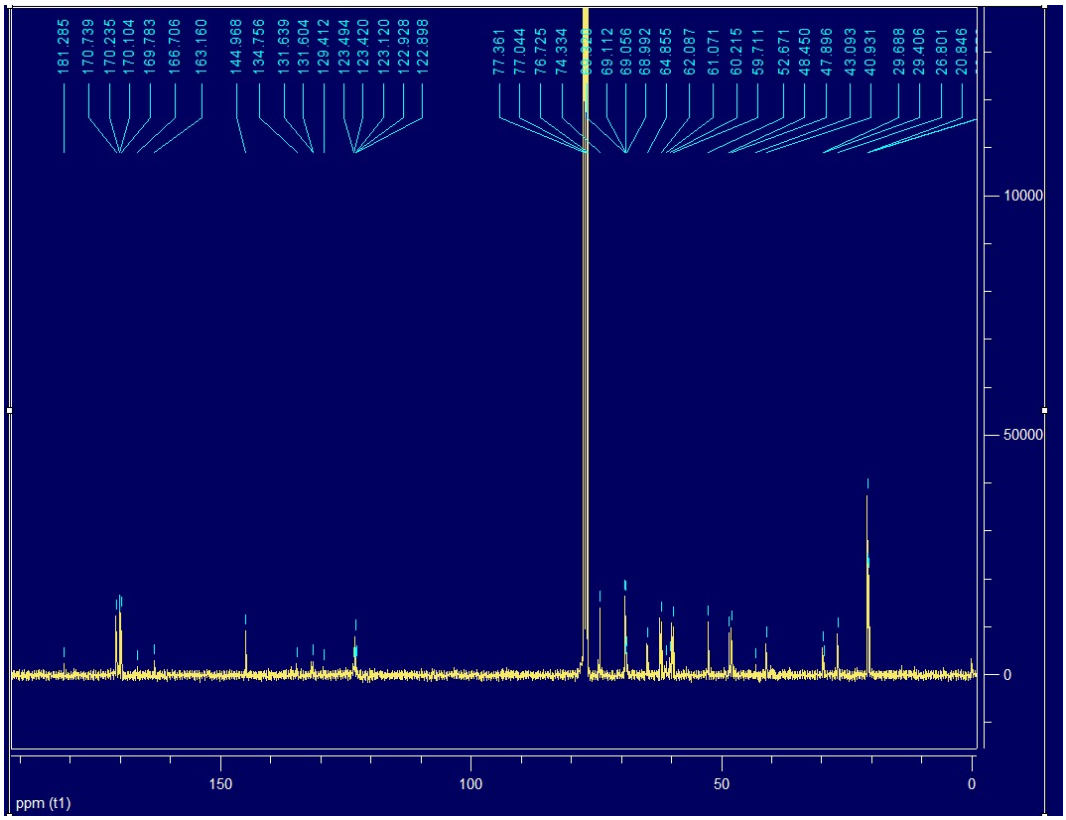

Fig. S15 ^{13}C NMR of compound **PBI-AcDNJ** ($CDCl_3$, 100 MHz).

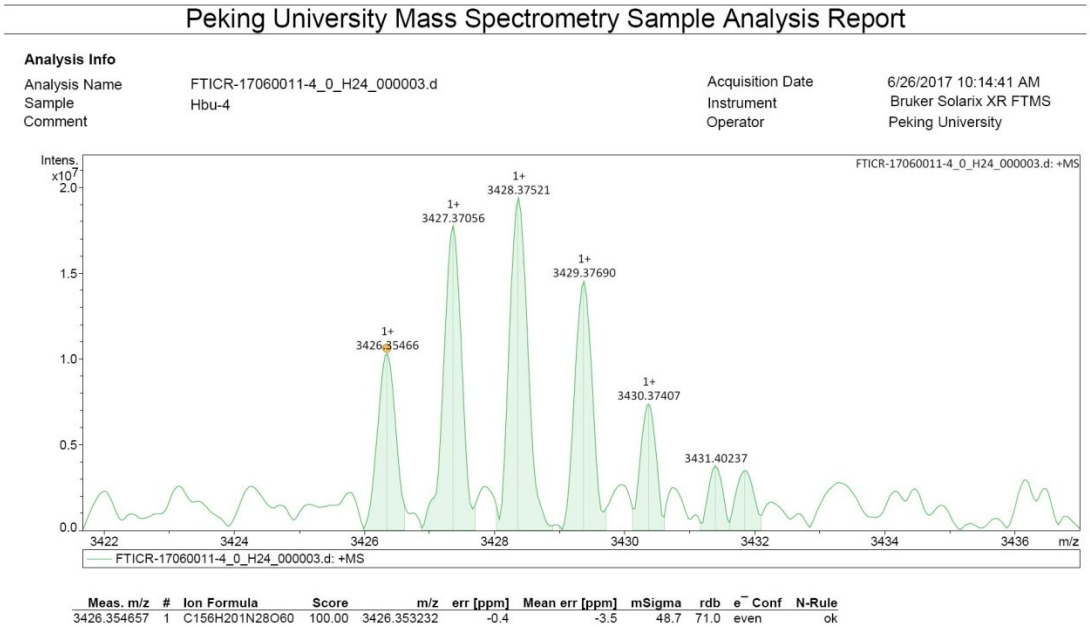

Fig. S16 HRMS of compound **PBI-AcDNJ**.

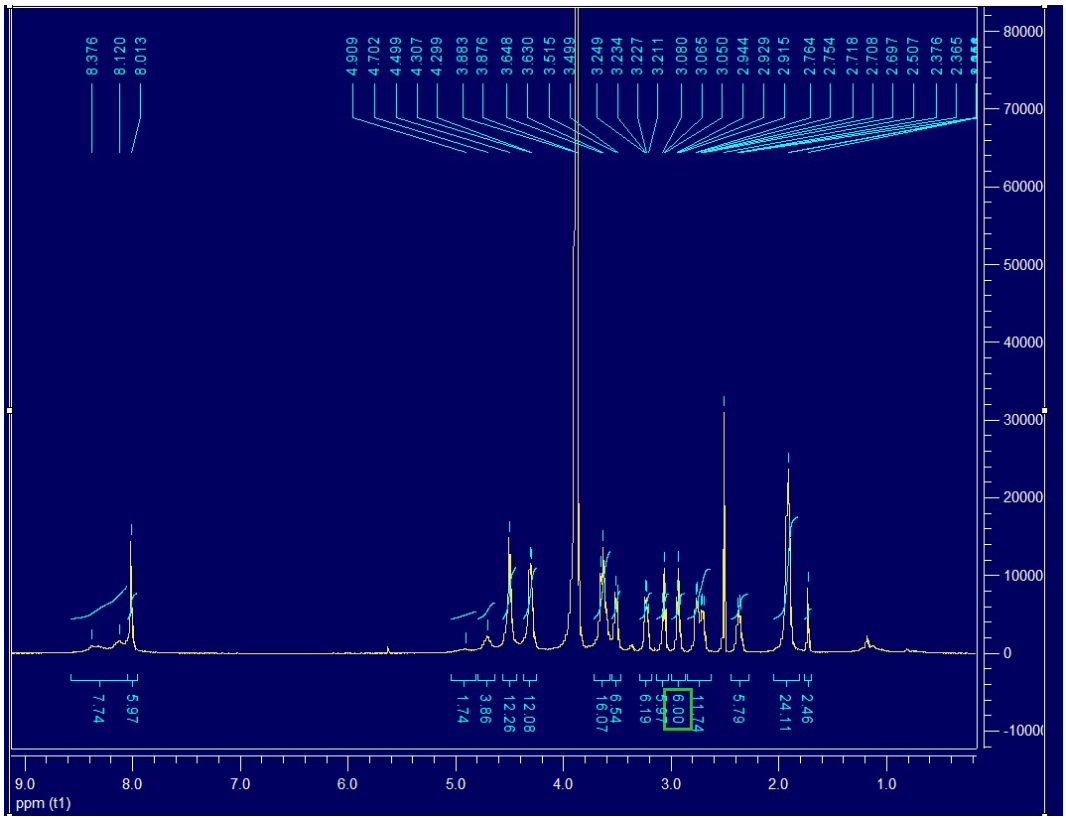

Fig. S17 ^{1}H NMR of compound **PBI-DNJ** (DMSO-d_6, 600 MHz).

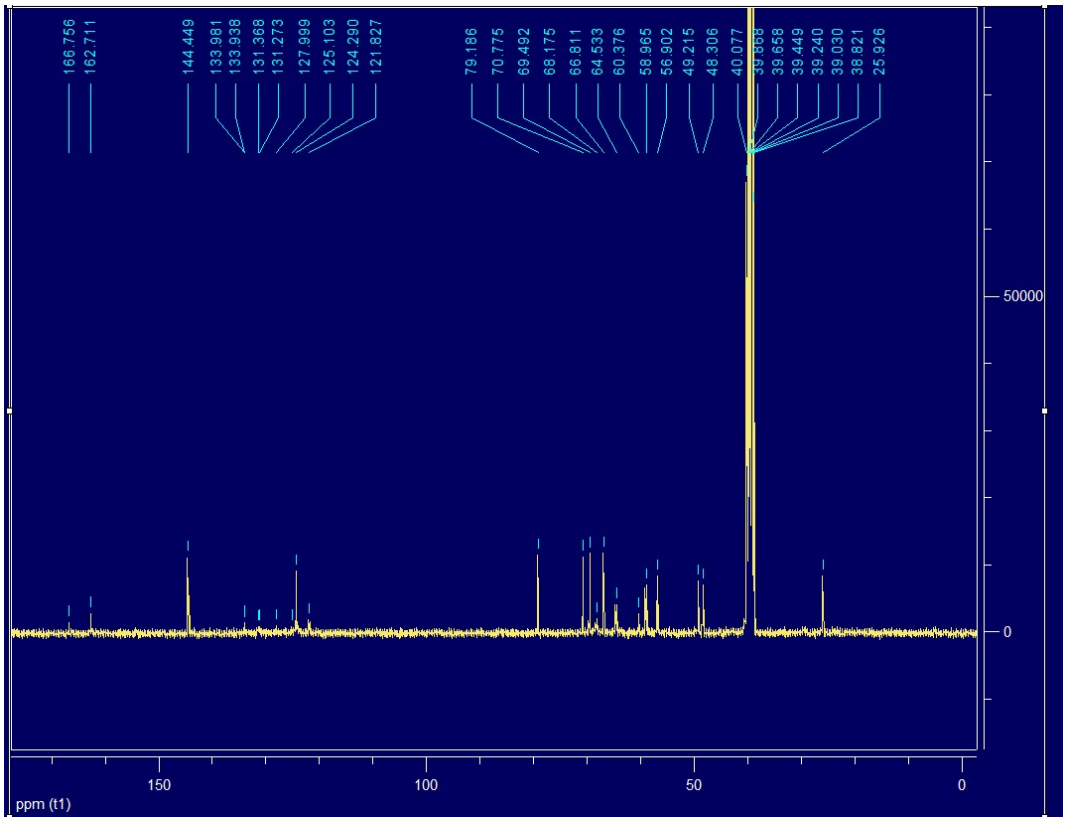

Fig. S18 ^{13}C NMR of compound **PBI-DNJ** (DMSO-d_6, 100 MHz).

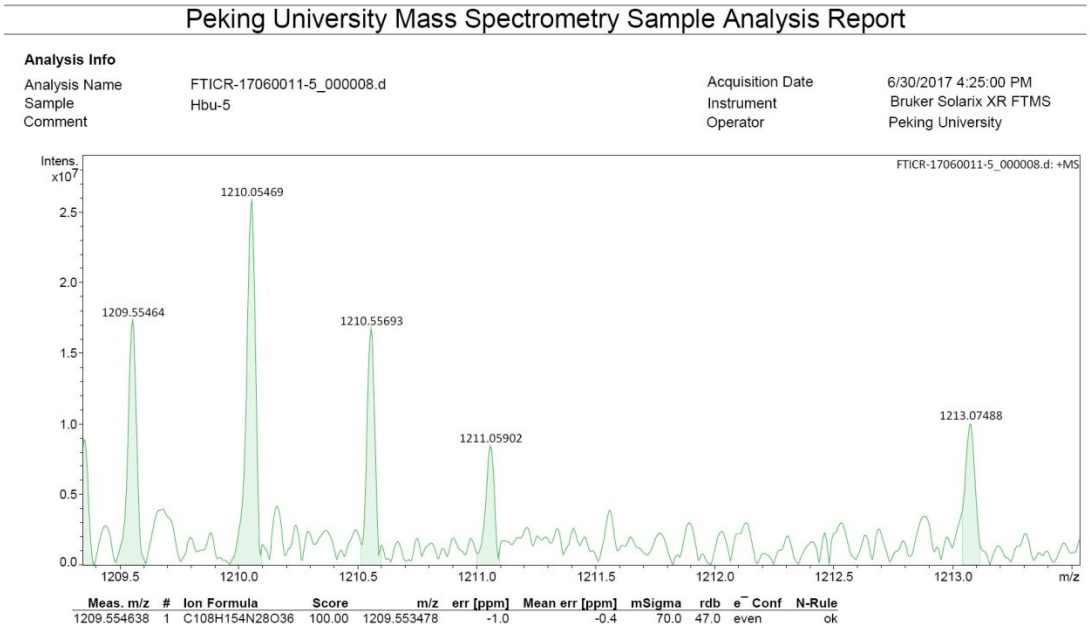

Fig. S19 HRMS of compound **PBI-DNJ**.

References

[1] Y. Brissonnet, C. O. Mellet, S. Morandat, M. I. G. Moreno, D. Deniaud, S. E. Matthews, S. Vidal, S. Šesták, K. E. Kirat and S. G. Gouin, *J. Am. Chem. Soc.*, 2013, **135**, 18427.

[2] J. Diot, M. I. García-Moreno, S. G. Gouin, C. O. Mellet, K. Haupt and J. Kovensky, *Org. Biomol. Chem.*, 2009, **7**, 357.

[3] E. Howard, A. Cousido-Siah, M. L. Lepage, J. P. Schneider, A. Bodlenner, A. Mitschler, A. Meli, I. Izzo, A. Alvarez, A. Podjarny and P. Compain, *Angew. Chem. Int. Ed.*, 2018, **57**, 8002.

[4] C. Decroocq, D. Rodríguez-Lucena, V. Russo, T. M. Barragán, C. O. Mellet and P. Compain, *Chem. Eur. J.*, 2011, **17**, 13825.

[5] J. F. Nierengarten, J. P. Schneider, T. M. N. Trinh, A. Joosten, M. Holler, M. L. Lepage, A. Bodlenner, M. I. García-Moreno, C. O. Mellet and P. Compain, *Chem. Eur. J.*, 2018, **24**, 2483.

[6] M. L. Lepage, J. P. Schneider, A. Bodlenner, A. Meli, F. D., Schmitt M., Tarnus C., Nguyen-Huynh N. T., Francois Y. N. Riccardis, E. L. Leize-Wagner, C. Birck, A. Cousido-Siah, A. Podjarny, I. Izzo and P. Compain, *Chem. Eur. J.*, 2016, **22**, 5151.

[7] C. Bonduelle, J. Huang, T. Mena-Barragán, C. O. Mellet, C. Decroocq, E. Etamé, A. Heise, P. Compain and S. Lecommandoux, *Chem. Commun.*, 2014, **50**, 3350.